Tethered UAV-Assisted Networks for Ubiquitous Near-shore Maritime Connectivity

Jichen Lu, Sahar Ammar, Osama Amin, Basem Shihada

Computer, Electrical and Mathematical Science and Engineering Division

King Abdullah University of Science and Technology (KAUST)

Thuwal, Makkah Prov., 23955, Saudi Arabia

{jichen.lu, sahar.ammar, osama.amin, basem.shihada}@kaust.edu.sa

Abstract-Recent years have witnessed an increase in maritime activities such as aquaculture, marine life monitoring and maritime tourism. However, due to the challenges associated with installing basic equipment at sea, network coverage and speed are subpar across the majority of the ocean. This limits the implementation of technologies requiring high throughput, including AI applications and extensive real-time data transfer. Although satellites can provide network coverage in remote regions, the service is expensive and constrained by a limited visibility window resulting in frequent handovers. Therefore, to provide higher capacity and larger coverage to the near-shore vessel users through terrestrial gateways, we propose a tethered Unmanned Aerial Vehicle (UAV)assisted maritime communication system. Additionally, we use a multi-hop relay strategy and apply a two-tier heuristic algorithm to optimize traffic routing and resource allocation while maximizing the system coverage. The proposed aerialmaritime system has been proven to enhance the throughput and coverage performance.

Index Terms—Aerial-maritime communication, tethered UAV, near-shore networks, multi-hop decode-and-forward relay.

I. INTRODUCTION

The marine environment covers around 71% of the Earth, yet most of its areas are unconnected due to the difficulty of deploying communication infrastructure on water. Concurrently, the rise of maritime activities has led to an increased demand for high communication services, such as real-time maritime monitoring systems and broadband communications, which require high throughput systems. Various solutions, including terrestrial, non-terrestrial, and hybrid networks, have been explored to cover the gap between the existing maritime communication technologies and the growing demand [1]–[3].

Traditionally, satellite communication has been the standard for marine vessel communications. Particularly, low earth orbit (LEO) satellites can offer tens of Mbps in data transfer rates. However, their high altitude and deployment costs present challenges such as high latency and significant expenses, respectively [1]. To enhance cost-effective network access for vessels, terrestrial LTE communication networks have been utilized to expand the coverage via vessel-to-vessel communications [4], [5]. However, the effectiveness of these methods is limited by the height of antennas on vessels, restricting their coverage range. Moreover, as a result of the duct layer effect [6]–[8], the system suffers from the sea surface, vessels and duct layer causing

inter-symbol interference, which can affect the operation of the maritime mesh network. To overcome these barriers, hybrid terrestrial-aerial networks have been developed to extend the coverage and provide service by exploiting the broad connectivity of aerial platforms, including balloons and unmanned aerial vehicles (UAVs), while benefiting from the low cost and latency of terrestrial networks [9]–[11]. Several UAV-based systems have been developed to provide on-demand maritime communication service for near-shore vessels [12]–[15]. Despite their flexibility and ease of deployment, UAVs suffer from limited endurance due to battery-charging limitation [16]. To address this issue, tethered UAVs emerge as a viable alternative, as they are easy to deploy and can fly for extended periods [14], [17].

Research solutions using tethered UAVs for near-shore communications have been proposed to improve coverage and throughput [12], [15], [18]. In [18], Fang *et al.* applied non-orthogonal multiple access on an integrated satellite-UAV-terrestrial network system to provide extended IoT connectivity across maritime environments. Other studies optimized the positioning of tethered UAVs along the shore to maximize coverage and data transmission capacity [12], [15]. To the best of our knowledge, existing research on tethered UAV-based maritime communications focuses solely on two-hop links, with no efforts toward developing multi-hop solutions.

In this paper, we build on our work in [15] and propose a multi-hop tethered UAV-assisted maritime communication system, aiming to enhance connectivity and extend coverage in near-shore maritime areas. Our system employs a network of tethered UAVs strategically deployed along the coastline and on vessels to act as relay points. Thanks to the tethered UAVs, communication between the UAVs will not suffer from signal reflections, as they are positioned above the duct layer. However, the communication links between the UAVs and the vessels may be subject to reflected signals from the sea surface, which can be mitigated using movable antenna arrays. Utilizing a decode-and-forward (DF) relaying scheme, these UAVs facilitate data transmission between the terrestrial network and maritime vessels. We approach the network design as an integrated optimization problem rather than a set of isolated clusters. Then, we develop a two-tier optimization algorithm to maximize

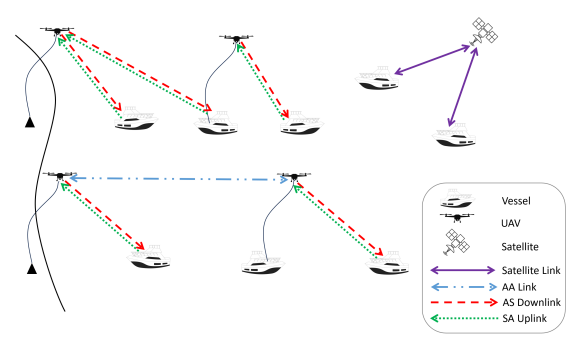


Fig. 1: Illustration of the tethered UAV-assisted maritime communication system.

the system's coverage. The simulation results validate the effectiveness of our proposed network solution, particularly in its capability to significantly expand the offshore service area.

II. SYSTEM MODELING

We propose an aerial-maritime hybrid communication system designed to enhance near-shore maritime connectivity through the deployment of two types of tethered UAVs. On the one hand, the tethered UAVs installed on the coastline act as gateway nodes to the core network. On the other hand, the tethered UAVs installed on the vessels act as relay nodes connecting the maritime vessels to the gateways, as depicted in Fig. 1. Our model conceptualizes a two-tiered communication framework, where the tethered UAVs constitute the aerial layer, and vessels form the sea surface. The system establishes intra- and interlayer communication links, facilitating connections within and between the two tiers. While satellite communication remains the default method for ensuring connectivity to distant vessels, our innovative multi-hop aerial-maritime hybrid system is specifically designed to expand the coverage of shore-based network access, consequently improving connectivity in coastal regions.

We consider both uplink and downlink, then the communication architecture incorporates three distinct types of links, denoted by $s \in \{AA, AS, SA\}$:

- Air-to-Air (AA): Link between tethered-UAVs.
- Air-to-Sea (AS): Downlink from a tethered-UAV to a vessel
- Sea-to-Air (SA): Uplink from a vessel to a tethered-UAV.

The curvature of the Earth's surface is a significant obstruction to maritime communication, often impeding direct line-of-sight (LOS) links. To circumvent this challenge, our system employs multi-hop relaying to facilitate connectivity for marine vessels that are unable to establish a direct link with shore-based nodes. Both tethered UAVs and marine vessels can serve as intermediate relays in this network, ensuring robust and extensive coverage.

We model the network as a graph in which the vessels and UAVs each represent a node, and we denote N as the set of all nodes. Each link from node a to node b is represented as $k \in \{(a,b) \mid a \in N, b \in N\}$. The positions of vessels

and UAVs are given by their Cartesian coordinates. The Euclidean distance between any two nodes is calculated as:

$$d_{k=(a,b)} = \sqrt{(x_a - x_b)^2 + (y_a - y_b)^2 + (h_a - h_b)^2}$$
 (1)

where x_i, y_i, h_i here are the x-coordinate, y-coordinate, height of node i, respectively, and d_k is the distance between the transmitter and the receiver.

To mimic the real-world situation, we adopt the distribution of vessels model based on the PDF in [19]:

$$f_{\rm R}^{\rm GEN}(r) = \frac{\mu \lambda^{b\mu}}{\Gamma(b)} r^{b\mu - 1} e^{-(\lambda r)^{\mu}}, r > 0$$
 (2)

where r is the distance between vessels, and we set constants as $b=0.6061, \mu=2.287, \lambda=11.9e^{-3}$ following Table 2(b)(1) in [19].

A. Channel Models

1) Large-scale Fading: Large-scale fading is affected by factors such as the position of the transmitter and the receiver, as well as the Earth's curvature, which can restrict the transmission distance to the LOS distance that is expressed as [20],

$$d_{\text{LOS},k=(a,b)} = \sqrt{h_a^2 + 2h_a R} + \sqrt{h_b^2 + 2h_b R},$$

$$h_a, h_b \in \{h_{\text{Vessel}}, h_{\text{UAV}}\},$$
(3)

where R is the radius of Earth in meters, h_a, h_b are heights of the transmitter and receiver.

a) Air-to-Sea Channel: The path loss of the Air-to-Sea channel can be modeled as [21],

$$L_{\rm AS}(d_k)|_{\rm dB} = A_{\rm AS} + 10\alpha_{\rm AS}\log_{10}\left(\frac{d_k}{d_{\rm min}}\right) + X_{\rm AS},$$

$$d_k \le d_{\rm LOS,k}$$
(4)

where $\alpha_{\rm AS}$ is the path loss exponent, $d_{\rm min}$ indicates the reference distance, $A_{\rm AS}$ is the path loss at the reference distance, $X_{\rm AS}$ is a Gaussian random variable representing the difference measurements and the mathematical model with $X_{\rm AS} \sim N(0, \sigma_{X_{\rm AS}}^2)$ [21].

b) Air-to-Air and Sea-to-Air Channels: We employ the free space path loss, which is suitable for high altitudes UAVs operating over the sea, to model the large-scale path loss for the Air-to-Air and Sea-to-Air channels [22] [23],

$$L_s(d_k)|_{\text{dB}} = 10\alpha_s \log_{10} \left(\frac{4\pi f d_k}{c}\right), s = \{AA, SA\},$$

$$d_k \le d_{\text{LOS},k}$$
(5)

where s is the link type, α_s is the path loss exponent, f is the carrier frequency, and c is the speed of light. Hence, the path gain of link k is expressed as,

$$g_{k=\{a,b\}} = 10^{-\frac{L_k - G_a - G_b}{10}} \tag{6}$$

where G_a and G_b are the antenna gain of the transmitter and the receiver, respectively.

2) Small-scale Fading: In the maritime environment, small-scale fading is induced by the weak paths caused by the numerous sea surface reflections, particularly in rough sea scenarios. Small-scale Fading is modeled as a Rician fading and defined by the following probability density function [24],

$$f_{\xi_k}(x) = \frac{x}{\sigma_k^2} \exp\left(\frac{-(x^2 + v_k^2)}{2\sigma_k^2}\right) I_0\left(\frac{xv_k}{\sigma_k^2}\right), x \ge 0 \quad (7)$$

where $2\sigma_k^2$ is the average received power of multipath components and v_k^2 is the received power of LOS component. $I_0(\cdot)$ denotes the first kind of modified Bessel function of the 0^{th} order defined as, $I_0(x) = \sum_{m=0}^{\infty}{(m!)^{-2}(x/2)^{2m}}$.

B. Average Capacity

For single-hop or multi-hop links serving node i, the instantaneous channel capacity C_i depends on both signal-to-noise ratio (SNR) and the number of hops, and it is defined as [25],

$$C_i = \frac{B}{M_i} \log_2(1 + \gamma_i) \tag{8}$$

where B is the bandwidth and M_i is the number of hops needed to reach node i, which varies depending on the selected path, and γ_i denotes the end-to-end instantaneous SNR. We apply DF relaying in our system, hence, γ_i depends on the minimum SNR along the link to the i-th node, which is computed from [26],

$$\gamma_i = \min_{j=1,\dots,M} \{\gamma_j\} \tag{9}$$

where γ_j is the instantaneous SNR for the j – th hop from node a to node b and is given by,

$$\gamma_{j=(a,b)} = \frac{P_a g_j |\xi_j|^2}{\sigma_N^2}$$
 (10)

where P_a is the transmitted power of node a, and σ_N^2 is the Gaussian noise power. Throughout our work, we assume negligible interference due to implementing a time-division multiple access (TDMA) scheme and an effective frequency reuse system across the service area.

To evaluate the system performance, we adopt the average capacity \hat{C}_i given by,

$$\hat{C}_i = \frac{B}{M_i} \mathbb{E}\left[\log_2(1+\gamma_i)\right]$$

$$= \frac{B}{M_i} \int_0^\infty \left(\log_2(1+x)\right)' (1-F_{\gamma_i}(x)) dx$$
(11)

where $\mathbb{E}[.]$ is the expectation operator and $F_{\gamma_i}(x)$ is the cumulative distribution function (CDF) of γ_i , expressed as,

$$F_{\gamma_i}(x) = 1 - \prod_{j=1}^{M} (1 - F_{\gamma_j}(x))$$
 (12)

Since we assume that ξ_j follows a Rician distribution where $\sigma_j^2=1$, then the SNR γ_j follows a non-central chisquared distribution with two degrees of freedom and noncentrality parameter v_j^2 . Then the CDF of γ_j is expressed as,

$$F_{\gamma_i}(x) = 1 - Q_1(v_i, \mu_i(x))$$
 (13)

where $v_j = \sqrt{P_a g_j}$ and $\mu_j(x) = \sqrt{(x\sigma_N^2)/(P_a g_j)}$. Thus, \hat{C}_i becomes

$$\hat{C}_{i} = \frac{B}{M_{i}} \int_{0}^{\infty} \left[\frac{1}{\ln(2)(1+x)} \left(\prod_{j=1}^{M} Q_{1}(v_{j}, \mu_{j}(x)) \right) \right] dx,$$
(14)

where $Q_1(a,b)$ denotes the Marcum Q-function of first order written as, $Q_1(a,b) = \int_b^\infty t \exp\left(-(t^2+a^2)/2\right) I_0(at)dt$, and $I_0(at)$ is modified Bessel function of first kind.

C. Upper Bound of Average Capacity

To obtain an upper bound for \hat{C}_i , we exploit the concavity of $\log_2(\cdot)$ and employ Jensen's inequality [27] obtaining,

$$\hat{C}_i \le \frac{B}{M_i} \log_2 \left(1 + \hat{\gamma}_i \right), \tag{15}$$

where $\hat{\gamma}_i = \mathbb{E}[\gamma_i]$.

III. TETHERED UAV-ASSISTED MARITIME COMMUNICATION NETWORK DESIGN

The system is designed to improve network coverage in near-shore maritime environments, thereby enhancing connectivity for marine vessels. Specifically, we focus on both uplink and downlink coverage in the scenario that one tethered UAV is located onshore as the source gateway. In our proposed design, the single source gateway provides service to vessels navigating near the coastline via single and multiple hops. This framework is designed with scalability in mind and can be adapted to configurations with multiple source gateways through the implementation of time division multiplexing and frequency reuse strategies. In the rest of this section, we will define the objective function, analyze it, and propose an algorithm for optimizing this function.

A. Problem Formulation

Our objective is to maximize the coverage of our system, which is defined by the number of vessels that achieve higher throughput using our system compared to existing satellite connections. For the purposes of this problem, a vessel is considered "covered" if it meets this criterion. We apply this objective to both uplink and downlink scenarios, and use footnote l to indicate variable for specific link direction, e.g. $\hat{C}_{i,l}$. The optimization problem can be formulated as follows:

$$\max_{v_{i,l}, n_{m_{i,l}}^{l}} |V_{S,l}| \tag{16a}$$

s.t.
$$w_{i,l}\hat{C}_{i,l} \ge C_{\text{sat},l}, l = \{U, D\}, \forall i \in V_{S,l}, (16b)$$

 $\{U, D\} |V_{S,l}|$

$$\sum_{l} \sum_{i} w_{i,l} = 1, \tag{16c}$$

$$j = \left(n_{m_{i-1,l}}^i, n_{m_{i,l}}^i\right),\tag{16d}$$

$$1 \le m_{i,l} \le M_{i,l},\tag{16e}$$

$$n_{m_{i,l}}^{i} \in V, \tag{16f}$$

where $V_{\rm S,l}$ denotes the set of vessels covered by our system, $\hat{C}_{i,l}$ represents the maximum estimated throughput for each vessel i in $V_{S,l}$, and $C_{\text{sat},l}$ is the benchmark throughput provided by satellite connections which variate for uplink U and downlink D. The resource allocation weight for vessel i is denoted by $w_{i,l}$, which is determined through the dedicated assignment of time and frequency resources achieving an estimated throughput of $w_{i,l}C_{i,l}$, which ensures orthogonal access. Each hop in the network is represented from $n_{m_{i-1},l}^i$ to $n_{m_{i,l}}^i$, where n_0^i is the source gateway and V is the set of all vessels within the network's range. The path to each vessel is uniquely defined as $n_{0,l}^i \to n_{1,l}^i \to \ldots \to n_{M_{i,l}}^i$, with $n_{0,l}^i$ as the source node.

B. Two-Tier Optimization Framework

The optimization problem previously defined is classified as mixed-integer nonlinear programming, stemming from the complexities involved in routing selection (discrete optimization) and resource allocation (continuous optimization). This problem is characterized by a discrete objective function and continuous nonlinear capacity constraints. To address this challenging problem, we propose a two-tier heuristic approach that decomposes it into two manageable sub-problems. In the first tier, we assume that each vessel has unrestricted access to the available resources, allowing us to concentrate on optimizing routing paths. The second tier focuses on the strategic allocation of resources among the vessels, ensuring that bandwidth is distributed in such a way that maximizes the number of vessels with improved connectivity.

1) Routing Optimization Tier: At this stage, we assume full resource allocation for each vessel. The objective is to maximize the throughput of each vessel independently, leading to the following simplified optimization problem:

$$\max_{n_{m_{i,l}}^{i}} |V_{S,l}| \tag{17a}$$

s.t.
$$\hat{C}_{i,l} \ge C_{\text{sat},l}, l = \{U, D\}, \forall i \in V_{S,l},$$
 (17b)

$$j = \left(n_{m_{i-1,l}}^i, n_{m_{i,l}}^i\right),\tag{17c}$$

$$1 \le m_{i,l} \le M_{i,l},\tag{17d}$$

$$n_{m_i}^i \in V, \tag{17e}$$

One heuristic idea is to iteratively use the vessel with maximum throughput to try to update other vessels, then remove the vessel from consideration. During the update, if the new path gets a higher average capacity for the vessel, we will update it. In this way, we guarantee that each vessel gets the optimal routing from the source. The correctness of this heuristic greedy algorithm can be proved by the monotonically decreasing of capacity during multihop: substituting (12) into (11), since $(1 - F_{\gamma_i}(x))$ is less than 1, \hat{C}_i decrease when M increase. Therefore, during the update process, we guarantee that all nodes with higher capacity will be used to update the specific nodes and select the path with maximum average capacity. The detailed algorithm is shown in Algorithm 1.

To reduce the unnecessary time spent on accurate integrals, we develop an upper bound used in the algorithm.

Using (15) to compute the upper bound of the average capacity from the new path to the node and compare as in Algorithm 1.16-21: if the upper bound is lower than the current average capacity of the node, then we do not need to calculate the accurate average capacity; otherwise, we calculate the accurate average capacity and make the comparison to decide whether update the node with the new path.

Algorithm 1 Optimal DF Relay-based Routing Algorithm

- 1: **Input:** $(x^{\text{Source}}, y^{\text{Source}}), (x_i^{\text{Vessel}}, y_i^{\text{Vessel}})$: nodes coordinates; T^{Source} : source type; U_i : binary variables to indicate UAV deployment; h_{UAV} , h_{Vessel} : height values; p_{UAV} , p_{Vessel} : power values; l: link direction.
- 2: **Output:** Maximum capacity $\hat{C}_{i,l}$ for each vessel.
- 3: **Initialization:** Create source node s with $(x^{\text{Source}}, y^{\text{Source}})$ and T^{Source} , then initialize: $\hat{C} = \infty$, $\hat{\gamma}^{\min}=0,\ M=0.$ Create vessel nodes n_i with $(x_i^{\mathrm{Vessel}},y_i^{\mathrm{Vessel}})$ and U_i , then initialize: $\hat{C}_{i,l}=0,$ $\hat{\gamma}_{i,l}^{\min}=0,\ M_{i,l}=0.$ Initialize max heap H, an empty
- 4: Begin:
- 5: Push nodes n_i into H. Use node s to update n_i in Hwith Eq.14 to update accurate average capacity.
- 6: **while** H is not empty **do** Pop the top node c in H and push it into F. 7: if $M_{c,l} == 0$ then 8: 9: Continue. 10: end if
- for Node m in H: do 11: $M'_{m,l} = M_{c,l} + 1,$ 12: 13:
- $\hat{\gamma}_{m,l}^{\min} = \min\left(\hat{\gamma}_{c,l}^{\min}, \frac{P_k h_k E\left[|\xi_k|^2\right]}{\sigma_{N_k}^2}\right),$ Get upper bound: $\hat{C}_{m,l}^{\max} = \frac{B}{M'_{m,l}} \log_2\left(1 + \hat{\gamma}_{m,l}^{\min}\right),$ 14: (Link type and heights depend on U_c , U_m and l) 15:
 - if $\hat{C}_{m,l}^{\max} \geq \hat{C}_{m,l}$ then
- Re-calculate accurate capacity $\hat{C}'_{m,l}$ with Eq.14. 17:
- $$\begin{split} \text{if } \hat{C}'_{m,l} & \geq \hat{C}_{m,l} \text{ then} \\ M_{m,l} & = M'_{m,l}, \ \hat{\gamma}^{\min}_{m,l} = \hat{\gamma}'^{\min}_{m,l}, \ \hat{C}_{m,l} = \hat{C}'_{m,l}. \end{split}$$
 18: 19: 20:
- end if
- 21:

16:

- end for 22:
- 23: end while
- 24: **End:** Get the capacity for each vessel $\hat{C}_{i,l}$ in set F.
- 2) Resource Allocation Tier: With $\hat{C}_{i,l}$ obtained for all vessels from the first stage, the next step is to optimize the resource allocation weight, as described by the following objective:

$$\max_{w_{i,l}} |V_{\mathrm{S},l}| \tag{18a}$$

s.t.
$$w_{i,l}\hat{C}_{i,l} \ge C_{\text{sat},l}, l = \{U, D\}, \forall i \in V_{S,l}$$
 (18b)

$$\sum_{l}^{\{\text{U,D}\}} \sum_{i}^{|V_{\text{S,l}}|} w_{i,l} = 1$$
 (18c)

$$V_{\rm S,1} \subset V$$
 (18d)

The second tier objective function is also discrete due to the need to select specific vessels for service. A heuristic method is employed to incrementally increase $|V_{\rm S,l}|$ from 0 to |V|, prioritizing vessels with the highest capacities for service and allocating more resources to those with lower throughput in the initial stage. We assume that the time slots are evenly divided for uplink and downlink. The resource allocation algorithm is elaborated in Algorithm 2.

Algorithm 2 Heuristic Resource Allocation Algorithm

- 1: **Input:** Vessel set V; average capacity $\hat{C}_{i,l}$ for each vessel; satellite capacity $C_{\text{sat},l}$.
- 2: Output: Served vessel set $V_{S,l}$; resource allocation weight $W_{\mathrm{S},l}=\{w_{i,l}\}$ for $i\in V_{\mathrm{S},l}$; maximum cardinality c of $V_{S,l}$.
- 3: **Initialization:** $V_{S,l} = \{\}; W_{S,l} = \{\}; c_l = 0.$
- 4: Begin:
- **for** n from 1 to |V| **do**
- Select vessels from V with top n $\hat{C}_{i,l}$ as V'. 6:

7: Assign weight
$$w_{i,l}=\frac{\frac{1}{|C_{i,l}|}}{2\sum\limits_{i}^{|V_{S,1}|}\frac{1}{|C_{i,l}|}}$$
 among V' .

- if $\min(w_{i,l}\hat{C}_{i,l}) < C_{\text{sat},l}$ then 8:
- 9:
- 10:

10: **else**
11:
$$V_{S,l} = V'; \ W_{S,l} = \{w_{i,l}\}; \ c_l = n.$$
12: **end if**

- 12:
- 13: end for
- 14: **End:** Return $V_{S,l}, W_{S,l}, c_l$.

3) Time Complexity Analysis: To find the vessel with maximum average capacity, we maintain a max heap (a data structure containing all nodes), which always has the vessel with maximum capacity as the top node. The construction of a max heap in Algorithm 1.5 spends $n \log_2(n)$. For n vessels we take $n \log_2(n)$. The update times will be the summation of left nodes each time. For resource allocation, still use max heap and traverse from 0 to n. The time complexity for the algorithm is calculated as follows:

$$T_{\text{routing}} = 2n \log_2(n) + \frac{(n+1)n}{2} + 2n \log_2(n) = O(n^2)$$
(19)

For the utilization of the upper bound, for each time of unnecessary update, we reduce the time complexity from O(M) to O(1), since we can store the minimum SNR along the path for each node.

IV. NUMERICAL RESULTS

We conducted various simulation scenarios involving one single tethered UAV on shore and multiple tethered UAVs attached to marine vessels. In a square area with 500 kilometers edges, 20 vessels were randomly generated using (2), along with random deployments of tethered UAVs on these vessels. We conducted 1000 different vessel distributions and performed 20 experiments for each distribution, with varying selections of vessels for tethered UAV deployment. The simulations are done for uplink and downlink scenarios. The simulation parameters are detailed

in Table I. Additionally, we consider the satellite system performance of Starlink's service and set downlink and uplink capacities to 100Mbps and 15Mbps, respectively [28].

TABLE I: Simulation Parameters

Parameter	Value
Height of UAV, h_{UAV}	200m
Height of Vessel, h_{Vessel}	4m [6]
Power of UAV, $P_{\rm UAV}$	30W [18]
Power of Vessel, P_{Vessel}	30W
Antenna Gain of UAV/Vessel, $G_{\mathrm{UAV/Vessel}}$	5dBi [29]
Carrier Frequency, f	5GHz
Bandwidth, B	200MHz
Air-Sea Propagation exponent, α_{AS}	1.9 dB [21]
Variance of $X_{\rm AS}$, $\sigma_{X_{\rm AS}}^2$	2.6^2 [21]
Air-Air Propagation exponent, α_{AA}	1.9 dB [22]
Sea-Air Propagation exponent, α_{SA}	2.51 dB [22]

To assess the coverage performance of our system, we define the "UAV deployment rate" as the percentage of vessels equipped with tethered UAVs, and the "service rate" as the percentage of vessels that achieve better data rate performance with our system compared to satellite connections within the region of interest. It should be noted that vessels with a capacity lower than the established thresholds will be served directly by satellites. The service rate is plotted against varying percentages of UAV-equipped vessels, as depicted in Fig. 2.

For both downlink and uplink, the scenario with tethered UAV on the shore gains better performance in service rate due to its higher platform to extend the service coverage. Service rate increment is more obvious for uplink along with increasing UAV deployment rate, which the high capacity threshold for downlink can cause. At the same time, the multi-hop strategy shows more beneficial influence for uplink, where the final service rate can reach around 70%.

To gain a more intuitive visualization of how our methods extend the coverage, we plot the maximum support distance versus UAV deployment rate, where the distance indicates the furthest vessel we can provide service surpassing the performance of satellites. From Fig.3, the maximum support distance by the system increases along with the UAV deployment rate. Tethered UAVs on vessels give the system around 50km extra coverage distance for downlink and around 100km extension for uplink. At the same time, the multi-hop strategy enhances the extension of the uplink by around 20km compared with the one-hop.

V. CONCLUSION

With the development of maritime activities, the demand for communication quality over the sea is increasing. However, the lack of communication equipment over the sea limits the network service throughput and coverage. We propose a multi-hop tethered UAV system over the vessels to provide service to users with higher throughput than satellites. We apply the multi-hop DF relay strategy and the greedy optimization algorithm to support network access for remote vessels. The system has been proven to gain extra capacity and enlarge the coverage for near-shore

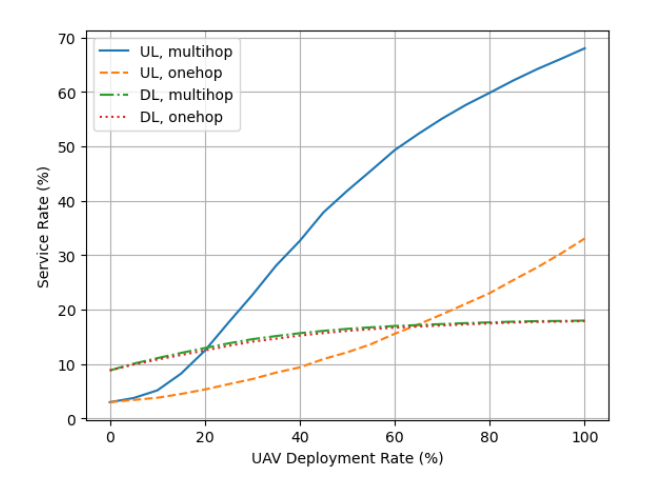


Fig. 2: Service Rate variations with UAV Deployment Rate.

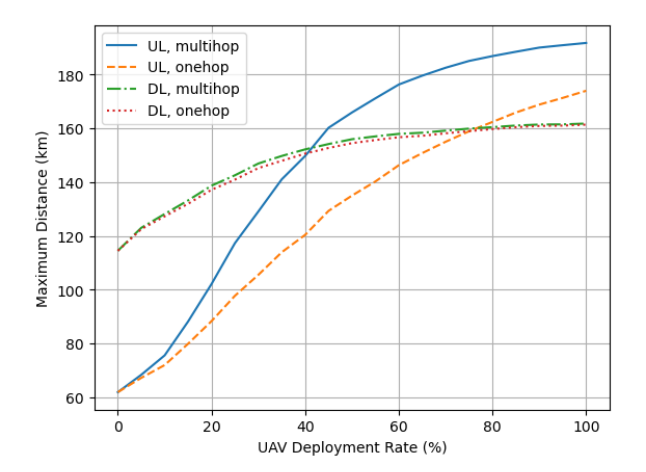


Fig. 3: Maximum Support Distance versus the UAV Deployment Rate.

communication scenarios through simulation results. In future work, we intend to explore the potential of optimizing UAV deployment and examine the system performance in dynamic scenarios, while considering environmental factors including wind and sea waves.

REFERENCES

- [1] F. S. Alqurashi, A. Trichili, N. Saeed, B. S. Ooi, and M.-S. Alouini, "Maritime communications: A survey on enabling technologies, opportunities, and challenges," *IEEE Internet Things J.*, Nov. 2022.
- [2] B. Shihada, O. Amin, C. Bainbridge, S. Jardak, O. Alkhazragi, T. K. Ng, B. Ooi, M. Berumen, and M.-S. Alouini, "Aqua-Fi: Delivering Internet underwater using wireless optical networks," *IEEE Commun. Mag.*, vol. 58, no. 5, pp. 84–89, 2020.
- [3] S. Ammar, C. P. Lau, and B. Shihada, "An in-depth survey on virtualization technologies in 6G integrated terrestrial and nonterrestrial networks," *IEEE Open J. Commun. Soc.*, vol. 5, pp. 3690– 3734, Jun. 2024.
- [4] H.-J. Kim, J.-K. Choi, D.-S. Yoo, B.-T. Jang, and K.-T. Chong, "Implementation of maricomm bridge for LTE-WLAN maritime heterogeneous relay network," in 17th Int. Conf. Advanced Commun. Technol. (ICACT), PyeongChang, South Korea, Jul. 2015, pp. 230– 234
- [5] S.-W. Jo and W.-S. Shim, "LTE-maritime: High-speed maritime wireless communication based on LTE technology," *IEEE Access*, vol. 7, pp. 53 172–53 181, Apr. 2019.
- [6] L. Yee Hui, F. Dong, and Y. S. Meng, "Near sea-surface mobile radiowave propagation at 5 GHz: measurements and modeling," *Radioengineering*, vol. 23, no. 3, pp. 824–830, Sep. 2014.

- [7] E. Dinc and O. B. Akan, "Channel model for the surface ducts: large-scale path-loss, delay spread, and AOA," *IEEE Trans. Antennas Propag.*, vol. 63, no. 6, pp. 2728–2738, Apr. 2015.
- [8] W. Wang, R. Raulefs, and T. Jost, "Fading characteristics of ship-toland propagation channel at 5.2 GHz," in OCEANS 2016-Shanghai, Apr. 2016, pp. 1–7.
- [9] R. Campos, T. Oliveira, N. Cruz, A. Matos, and J. M. Almeida, "BLUECOM+: Cost-effective broadband communications at remote ocean areas," in *OCEANS 2016-Shanghai*, Apr. 2016, pp. 1–6.
- [10] N. Nomikos, P. K. Gkonis, P. S. Bithas, and P. Trakadas, "A survey on UAV-aided maritime communications: Deployment considerations, applications, and future challenges," *IEEE Open J. Commun. Soc.*, vol. 4, pp. 56–78, Nov. 2022.
- [11] J. Lu, O. Amin, and B. Shihada, "Task-aware offloading for cloud computing in sky-based aerial data centers," *TechRxiv*, Aug. 2025, preprint. [Online]. Available: https://doi.org/10.36227/ techrxiv.175615804.41945749/v1
- [12] Y. Wang, X. Fang, W. Feng, Y. Chen, N. Ge, and Z. Lu, "On-demand coverage for maritime hybrid satellite-UAV-terrestrial networks," in Int. Conf. Wireless. Commun., Signal Process. (WCSP), Nanjing, China, Oct. 2020, pp. 483–488.
- [13] S. Guan, J. Wang, C. Jiang, R. Duan, Y. Ren, and T. Q. Quek, "MagicNet: The maritime giant cellular network," *IEEE Commun. Mag.*, vol. 59, no. 3, pp. 117–123, May 2021.
- [14] A. Kourani and N. Daher, "Marine locomotion: A tethered UAV-buoy system with surge velocity control," *Robot. Auton. Syst.*, vol. 145, p. 103858, Nov. 2021.
- [15] S. Ammar, O. Amin, and B. Shihada, "Tethered UAV-based communications for under-connected near-shore maritime areas," in *IEEE Int. Black Sea Conf. Commun. Netw. (BlackSeaCom), Tbilisi, Georgia*, Jun. 2024, pp. 42–47.
- [16] Z. Pan, L. An, and C. Wen, "Recent advances in fuel cells based propulsion systems for unmanned aerial vehicles," *Applied Energy*, vol. 240, pp. 473–485, Apr. 2019.
- [17] B. E. Y. Belmekki and M.-S. Alouini, "Unleashing the potential of networked tethered flying platforms: Prospects, challenges, and applications," *IEEE Open J. Veh. Technol.*, vol. 3, pp. 278–320, May 2022.
- [18] X. Fang, W. Feng, Y. Wang, Y. Chen, N. Ge, Z. Ding, and H. Zhu, "NOMA-based hybrid satellite-UAV-terrestrial networks for 6G maritime coverage," *IEEE Trans. Wireless Commun.*, vol. 22, no. 1, pp. 138–152, Jul. 2022.
- [19] G. Galati, G. Pavan, F. De Palo, G. Ragonesi et al., "Maritime traffic models for vessel-to-vessel distances." in VEHITS, Apr. 2016, pp. 160–167.
- [20] W. Wang, R. Raulefs, and T. Jost, "Fading characteristics of maritime propagation channel for beyond geometrical horizon communications in C-band," CEAS Space J., vol. 11, pp. 95–104, Mar. 2019.
- [21] D. W. Matolak and R. Sun, "Air-ground channel characterization for unmanned aircraft systems—part I: Methods, measurements, and models for over-water settings," *IEEE Trans Veh. Technol.*, vol. 66, no. 1, pp. 26–44, Feb. 2016.
- [22] A. A. Khuwaja, Y. Chen, N. Zhao, M.-S. Alouini, and P. Dobbins, "A survey of channel modeling for UAV communications," *IEEE Commun. Surv. Tutor.*, vol. 20, no. 4, pp. 2804–2821, Jul. 2018.
 [23] N. Goddemeier and C. Wietfeld, "Investigation of air-to-air channel
- [23] N. Goddemeier and C. Wietfeld, "Investigation of air-to-air channel characteristics and a UAV specific extension to the Rice model," in *IEEE Global Commun. Conf. Workshops, California, USA*, Dec. 2015, pp. 1–5.
- [24] J. Wang, H. Zhou, Y. Li, Q. Sun, Y. Wu, S. Jin, T. Q. Quek, and C. Xu, "Wireless channel models for maritime communications," *IEEE Access*, vol. 6, pp. 68 070–68 088, Nov. 2018.
- [25] S. S. Ikki and M. H. Ahmed, "Performance analysis of best-path selection scheme for multi-hop amplify-and-forward relaying," *Eur. Trans. on Telecommun.*, vol. 21, no. 7, pp. 603–610, Nov. 2010.
- [26] Y. Chen, N. Zhao, Z. Ding, and M.-S. Alouini, "Multiple UAVs as relays: Multi-hop single link versus multiple dual-hop links," *IEEE Trans. Wireless Commun.*, vol. 17, no. 9, pp. 6348–6359, Aug. 2018.
- [27] J. L. W. V. Jensen, "Sur les fonctions convexes et les inégalités entre les valeurs moyennes," *Acta Math.*, vol. 30, no. 1, pp. 175–193, Dec. 1906.
- [28] "Starlink business maritime," https://www.starlink.com/bs/business/maritime, accessed: 2024-3-18.
- [29] R. Sun and D. W. Matolak, "Air–ground channel characterization for unmanned aircraft systems part II: Hilly and mountainous settings," *IEEE Trans. Veh. Technol.*, vol. 66, no. 3, pp. 1913–1925, Jun. 2016.